https://doi.org/10.31891/2307-5732-2025-349-67
УДК 621.3:681.34

**ЧЕРЕПАНОВ ІЛЛЯ**
Національний аерокосмічний університет ім. М.Є. Жуковського
"Харківський авіаційний інститут"
e-mail: c.illia@student.khai.edu

# ДОСЛІДЖЕННЯ РІЗНИХ МЕТОДІВ ВИБОРУ ПОРОГУ ДЛЯ DCT-SSA ФІЛЬТРУ

*Радар із синтетичною апертурою (SAR) використовуються для створення зображень, які застосовуються для різних практичних цілей, від аналізу ґрунту і рослинного покриву до пошуку великих скупчень незаконно скинутого сміття. Проблема в обробці таких зображень полягає в тому, що отримані зображення спотворюються спеклом - шумоподібним ефектом мультиплікативної природи. Крім того, спекл зазвичай має негаусівський розподіл і є просторово корельованим. Для покращення якості SAR-зображень було розроблено багато фільтрів, які враховують негаусівський розподіл і добре пригнічують спекл, наприклад, фільтри на основі дискретного косинусного перетворення (DCT) або BM3D-фільтри. Загальною проблемою більшості фільтрів залишається те, що вони спотворюють дрібні деталі, краї великих об'єктів і текстури, що призводить до небажаного ефекту розмиття. У цій статті перевіряється припущення, що, змінюючи тип порогу та метод його обчислення для блоків зображення, можна досягти кращого збереження точкових об'єктів та інших інформативних ознак. Представлено результати дослідження з використанням визначення локального порогу з обчисленням середнього, медіани та мінімальної інтерквантильної відстані для жорсткого та комбінованого порогів. За основу обрано фільтр DCT-SSA, оскільки DCT має добрі декореляційні властивості, а сам фільтр неодноразово демонстрував досить високу ефективність придушення спекл-спектрів. Як метрики якості використано PSNR, PSNR-HVS-M та HaarPSI, де остання вперше застосована для оцінки ефективності фільтрації SAR-зображень. Дані, отримані в цьому дослідженні, вказують на те, що запропоновані модифікації призводять до кращого збереження яскравих точок на зображенні і можуть бути використані для покращення якості зображення на виході ДКП-фільтра.*

*Ключові слова: Радар із синтетичною апертурою (SAR), метрики якості, PSNR-HVS-M, HaarPSI, ДКП-фільтри.*

**CHEREPANOV ILLIA**
National Aerospace University – Kharkiv Aviation Institute

# INVESTIGATION OF DIFFERENT METHODS OF THRESHOLD SELECTION FOR DCT-SSA FILTER

*Synthetic aperture radars (SARs) are used to acquire images that are employed for a variety of practical applications, from analyzing soil and vegetation cover to searching for large accumulations of illegally dumped debris. The problem of processing such images is that the obtained images are spoiled by speckle - a noise-like effect with multiplicative nature. Also, speckle has a non-Gaussian distribution and is spatially correlated. To address this problem, many filters have been developed that take into account the non-Gaussianity of the distribution and also provide acceptable speckle suppression. Discrete Cosine Transform (DCT) based filters or BM3D filters are examples of such filters. A common problem with most filters remains that they distort low-size details, edges of large-size objects and textures, resulting in an undesirable blurring effect. This paper tests the assumption that by changing the type of threshold and the method of its calculation for image blocks, it is possible to achieve improved preservation of point-like objects and other informative features. The results of a study using determination of the local threshold with calculation of mean, median and minimum interquantile distance for hard and combined thresholds are presented. The DCT-SSA filter is chosen as the basis, since DCT has good decorrelation properties, and the filter itself has repeatedly demonstrated quite high speckle suppression efficiency. PSNR, PSNR-HVS-M and HaarPSI are used as quality metrics, where the latter one is first applied to evaluate the efficiency of SAR image filtering. The data obtained in this study indicates that the proposed modifications result in better preservation of bright points in the image and can be used to improve the image quality of the DCT filter output.*

*Key words: Synthetic aperture radar (SAR), quality metrics, PSNR-HVS-M, HaarPSI, DCT-based filters.*

## Problem statement

SAR is a technology that uses active sensors to acquire high-resolution images of the Earth's surface by irradiating waves and processing the backscattered signal to form an image [1]. The main advantage of SAR sensors is their ability to acquire data regardless of the time of day or weather [2]. One of the main drawbacks of SAR technology is speckle [3, 4], a noise-like phenomenon present in all types of these images, which limits the measurement accuracy and the reliability of extracting useful information from SAR images. The need for effective speckle suppression in SAR images is mentioned in many papers [5, 6]. Many different filters belonging to different groups have been developed to solve this problem: from those using sliding window [7] to filters based on orthogonal transforms [8] and modern non-local approaches [9-11]. Various quality metrics are used to evaluate their performance [12-15]. The filtering performance tends to improve as shown by various quantitative metrics, improvements in image detail preservation and speckle suppression are demonstrated. Despite the progress that has been made in the development of new speckle suppression techniques, the selection of filter parameters that strike a balance between speckle suppression and preservation of object boundaries and fine details remains a challenge. The use of most current methods results in smoothing of the image in heterogeneous regions, which may lead to loss of information critical for further image processing. In order to fully utilize the potential of existing methods, it is necessary to provide better preservation of bright points (fine details), which is consistent with the visual quality requirements of the images. One of quite effective methods of speckle noise suppression is the DCT-SSA filter, which uses DCT in fixed-size blocks [16]. This filter can account for the spatial correlated nature of speckle as well as its multiplicative nature. One of the parameters of this filter is β, which is used to calculate the local value of the hard threshold in blocks, where the recommended (compromise) value is β=2.7. Increasing β can improve speckle suppression but causes to lose fine details in the image. Because of this, we can observe either a slight improvement of peak signal-to-noise ratio (PSNR) or its deterioration at the filter output. The improvement or degradation depends on the amount of fine detail in the image. In particular, it is shown in [17] that as the texture content of the image processed by the DCT-SSA filter increases, the output image quality decreases. Having analyzed the performance of this filter, we can suggest that changing the methodology for calculating the threshold value for an image block can help to achieve a better compromise between the preservation of edges, small-sized objects and textures and the degree of noise suppression.

**Analysis of recent sources**

One of the most common filters is the Lee filter [19]. The filter uses the principle of minimizing the MSE criterion for noise removal and relies on the assumption that the speckle present in the image has spatially invariant properties. This assumption may not be valid for images of rapidly changing areas and neighborhoods of bright points, resulting in loss of information due to blurring the object edges. The disadvantages of the classical Kuan filter [20] are similar. Another variant of speckle suppression, often implemented in software packages, is the Boxcar filter [21]. The filter is characterized by simplicity and high performance, but it tends to blur edges and fine details of the image, especially when using large windows, which limits its effectiveness in areas with high concentration of textures. For better speckle filtering, the SRAD [22] (Speckle reducing anisotropic diffusion) filter was developed, which can be considered an edge-sensitive version of classical speckle filters. This filter outperforms adaptive filtering methods developed with additive models in mind, but it also blurs the edges and small-sized objects. Because the speckle suppression operations for filters that are based on orthogonal image transformations are performed in the spectral domain, they can be more effective for speckle suppression. And after the transformations, the image can be easily, using fast algorithms, transformed back into the spatial domain again. The use of such filters allows providing better suppression of spatially correlated noise and preservation of fine image details. An example of such filters can be filters based on wavelet transforms, such as the Bilateral filter proposed in [23]. Also examples of such filters are the standard DCTF [24] and BM3D [25] filters, which use a hard threshold independent of frequency. These filters have proven to be among the best filters when dealing with additive white Gaussian noise, but when dealing with spatially correlated noise, such as speckle, their performance drops significantly. Another option for dealing with speckle in an image may be to combine classical methods with some new technique, such as the method proposed in [26]. The essence of the method consists in removing object edges before processing and adding them afterwards. The method has shown good results when working with the Lee filter, SRAD filter and filter based on wavelet transformations. However, only ultrasound images are considered in the work [26].

Many filters cannot be directly adapted to suppress spatially correlated noise, which may limit their use. Therefore, we consider below the DCT-based filters [18], which can be easily adapted to both the multiplicative nature and spatial correlation of speckle. In [17], the properties of spatially correlated noise in images acquired from Sentinel-2A and TerraSAR-X satellites were analyzed. Homogeneous areas, which presumably contain mainly noise, were identified in the images and their spectrum in the DCP domain was obtained. Using the data obtained in the course of the analysis on the degree of noise correlation in real images, in [17, 19] a method of generating this noise for test images and the noise correlation index $\sigma_G$ were proposed. With the parameter $\sigma_G <$ 0.5, the noise can be assumed to be pure white, when the parameter is in the interval $0.8 < \sigma_G < 1$, the noise can be considered to be weakly correlated, when the parameter is in the interval $1 < \sigma_G < 1.5$ it is possible to consider that the noise is moderately correlated and at $\sigma_G > 1.5$ the noise can be considered highly correlated. Modern methods for suppression of additive white Gaussian noise (AWGN) and spatially correlated noise with weak correlation were applied to the generated noise in [17]. As a result, it was found that the use of such filters is appropriate only for either images with a moderate degree of spatial correlation or for images with simple structure. A better filter was proposed in [16] based on DCT with adaptation to spatially correlated noise (SSA). The essence of the modification is to use a hard threshold value, which for each block is calculated by the following formula

$$T(n,m,k,l) = \beta\sigma_\mu \bar{I}(n,m)\sqrt{W(k,l)} \quad (1)$$

where β is the parameter controlling the filter properties, it is usually equal to 2,7; $\bar{I}(n,m)$ denotes the local mean for the image block with the upper left corner in the pixel with indices $n$, $m$; $\sigma_\mu^2$ is the relative variance of multiplicative noise (speckle); $W(k,l)$ denotes the normalized power DCT spectrum for the kl-th spatial frequency (further we assume that the 8×8 sliding block is used). Using a hard threshold means that if $|D(n,m,k,l)| \geq T(n,m,k,l)$, then the value of $D(n,m,k,l)$ remains unchanged, otherwise $D(n,m,k,l) = 0$. In the further modeling, we will be guided by the speckle characteristics typical for SAR images generated by the Sentinel-1 satellite system. As a basis, we will use the DCT-SSA filter based on formula (1) and its modifications.

**Presentation of basic material**

Let us consider the basic principle of operation of the DCT-filter. To use this filter (see (1)), one needs to know or estimate W(k,l) a priori. Usually, to obtain such estimates, one selects large homogeneous areas, which can be done either by an experienced operator or by one and specially developed algorithms. The selection of such areas is necessary because they contain pure noise without useful information, so that the DCT spectrum can be estimated and normalized. An example is shown in Figure 1. As can be seen from Figure 1 b), the spatially correlated noise in the spectral domain of the DCT is concentrated in the low spatial frequency region.

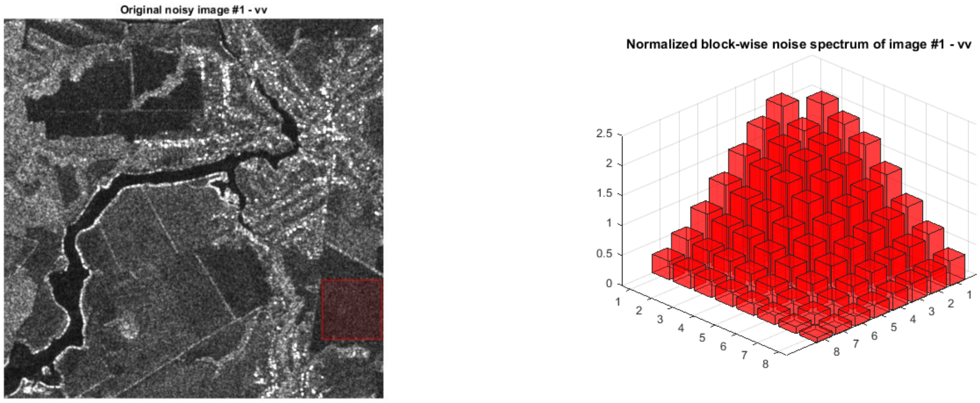


(a) (b)

**Fig.1 Obtaining noise parameters: a) - SAR image distorted by spatially correlated noise with selected homogeneous area marked by red square; b) - normalized noise spectrum**

Filtering is performed in four stages. At the first one, two-dimensional DCT is performed in each block, at the second - threshold processing is applied, for example, according to (1), at the third - inverse DCT with obtaining filtered values for each pixel of the block is carried out, at the fourth - aggregation of filtered values for each pixel is performed, if block overlapping is used. In the following, a variant of processing using 8x8 pixel blocks with full block overlap is considered. As can be seen from (1), the thresholds are proportional to $\bar{I}(n,m)$. In this regard, the presence of bright points in the block that have a positive contrast compared to their surrounding background leads to $\bar{I}(n,m)$ to be larger than most image values belonging to the background. This can lead to the problem of preserving bright points and small objects of 5-15 pixels in size. A similar problem occurs for blocks capturing contrast edges, leading to their over-smoothing. Our proposed modifications are based on the assumption that the choice of local mean $\bar{I}(n,m)$ to calculate the thresholds (formula (1)) for an image block may not be the best solution and it is potentially possible to obtain a better result by replacing the local mean with another local estimate of the background level. The modification we propose is to use the minimum interquantile distance, which is a good estimate of the mode of the distribution of values in the block. The principle of its calculation is as follows: form the sample y(s), s=1,…,64, of the pixel values belonging to a given block; sort them in ascending order and get order statistics $y^{(1)}$, $y^{(2)}$, …, $y^{(64)}$. Calculate differences of ordinal statistics $\Delta_1 = y^{(1+q)} - y^{(1)}$, $\Delta_2 = y^{(2+q)} - y^{(2)}$, …, $\Delta_{64\text{-}q} = y^{(64)} - y^{(64\text{-}q)}$, where q is the estimation parameter, equal to 32 in this case. Then find the smallest value Δ. For order statistics corresponding to this Δ, find the average value of $Iqr(n,m)$ for the block with upper left corner in the pixel with indices $n$, $m$. As a result, the threshold values are calculated as follows:

$$T(n,m,k,l) = \beta\sigma_{\mu} Iqr(n,m)\sqrt{W(k,l)}. \quad (2)$$

Additionally, we also check the possibility of replacing the local mean by the sample median $y(s)$, $s$=1,...,64 to calculate the threshold value:

$$T(n,m,k,l) = \beta\sigma_{\mu} M(n,m)\sqrt{W(k,l)} \quad (3)$$

where $M(n,m)$ is the median for the image block with the upper left corner in pixel with indices $n$, $m$.

The quality metrics chosen are the traditional PSNR at the filter output and two metrics that take human vision system (HVS) into account and characterize the loss (or preservation) of fine details in the image: the PSNR-HVS-M [27] and the recently proposed HaarPSI metric [28], which is based on visual attention maps. The first metric is a modification of the metric PSNR-HVS that accounts for the contrast sensitivity function. The second metric works on the principle of image similarity. Its main idea is to evaluate the similarity between two images by taking into account the human point of view. For PSNR and PSNR-HVS-M metrics, the larger the output value, the higher the filtering quality (both metrics are expressed in dB). HaarPSI values vary from -1 (images are not similar) to +1 (images are identical). As the test image, we use the image in Fig. 3,a, to which we added speckle noise with the same statistical ( $\sigma_{\mu}^2 = 0{,}05$) and spatial spectral (Fig. 1,b) characteristics as for the SAR images of the Sentinel-1 system. Since different values of β may be optimal for different methods of estimating the mean in blocks and different image content, we calculate the values of metrics for the range of their values from 2 to 4.2. The results are presented in Fig. 2.

As we can see, for each of the variants, the maximum quality is observed at different values of β. At the same time, according to the PSNR metric, the result for the calculation using the median (3) is better than for the other two variants.

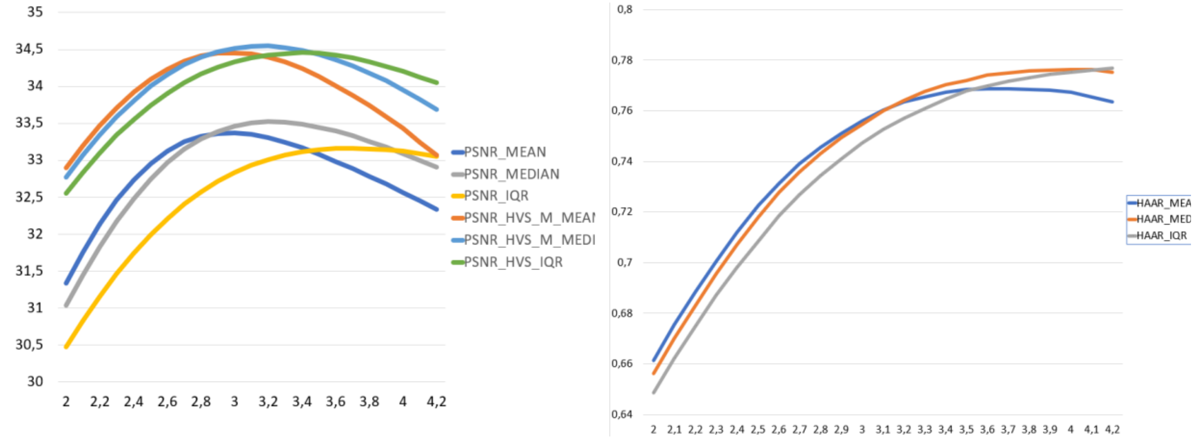


**a) б)**

**Fig.2 - Plots of dependence of PSNR and PSNR-HVS-M (a) and HaarPSI (b) on β for the image in Fig. 3,a**

The analysis of HaarPSI metric shows the following. Optimal values of β are also observed for it, while for the initial variant (1) $\beta_{opt} = 3.4$, for the modification using the median $\beta_{opt} = 3.8$, and for the variant (2), the maximum is observed for $\beta = 4.2$. For the PSNR-HVS-M metric, the maximum quality is achieved at $\beta_{\text{optimal}}^{\text{standard}} = 2.7$ for the original variant (1), for the modification using the median (3), $\beta_{\text{optimal}}^{\text{median}} = 3.2$, and for the modification using the minimum interquantile distance (2) at $\beta_{\text{optimal}}^{\text{IQR}} = 3.7$. The metric analysis shows that we achieve the best quality using the median (3). Let us look at the images that correspond to the best quantitative performance for each filter variant according to the PSNR-HVS and HaarPSI metrics (Figures 3 and 4).

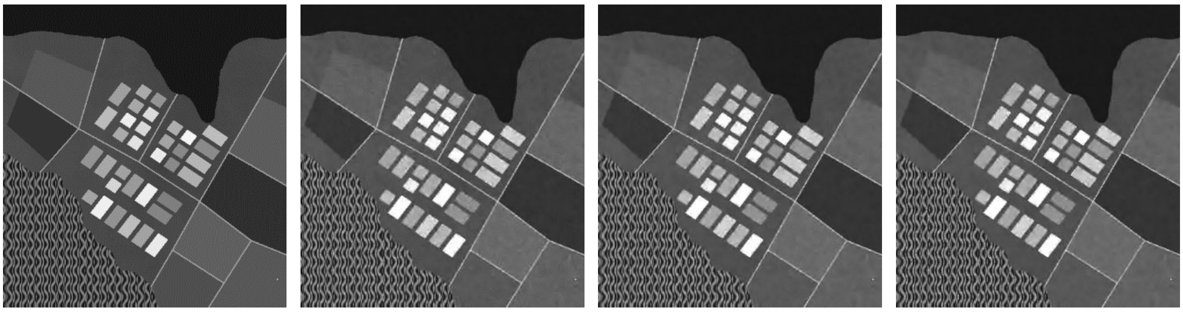

**a) b) c) d)**

**Fig. 3 Optimal images according to the PSNR-HVS-M metric: (a) - original image; (b) - original filter variant at the $\beta_{\text{optimal}}^{\text{standard}} = 2.7$; c) – A modification that uses the median at $\beta_{\text{optimal}}^{\text{median}} = 3.2$; d) – modification using the interquantile distance for $\beta_{\text{optimal}}^{\text{IQR}} = 3.7$**

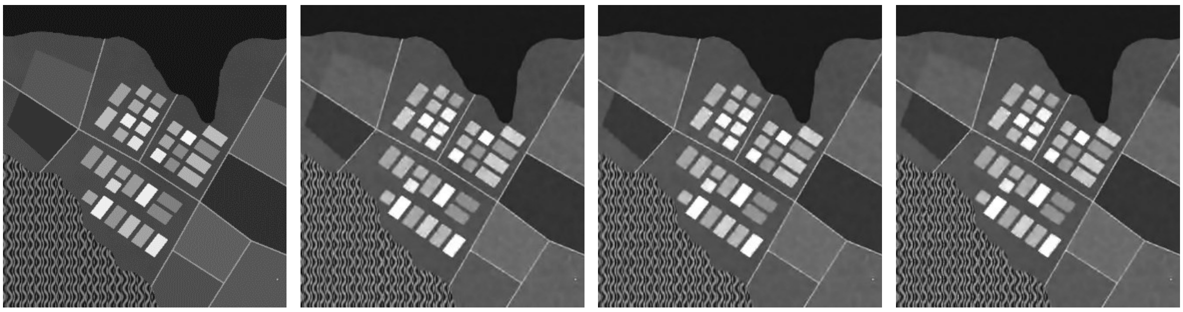

**a) b) c) d)**

**Fig. 4 Optimal images according to the HaarPSI metric: a) - original image; b) - original filter variant at $\beta_{\text{optimal}}^{\text{standard}} = 3.4$; c) – A modification that uses the median at $\beta_{\text{optimal}}^{\text{median}} = 3.8$; d) – modification using the interquantile distance for $\beta_{\text{optimal}}^{\text{IQR}} = 4.2$**

It is visually noticeable that in images with higher β the edges of objects appear more blurred, but we cannot say exactly what happens in bright points neighborhoods. For this purpose, let us perform an additional analysis by adding a simulated bright point - a cross consisting of 5 pixels - to the lower right corner and see how the bright point looks like at optimal β values for different filter variants.

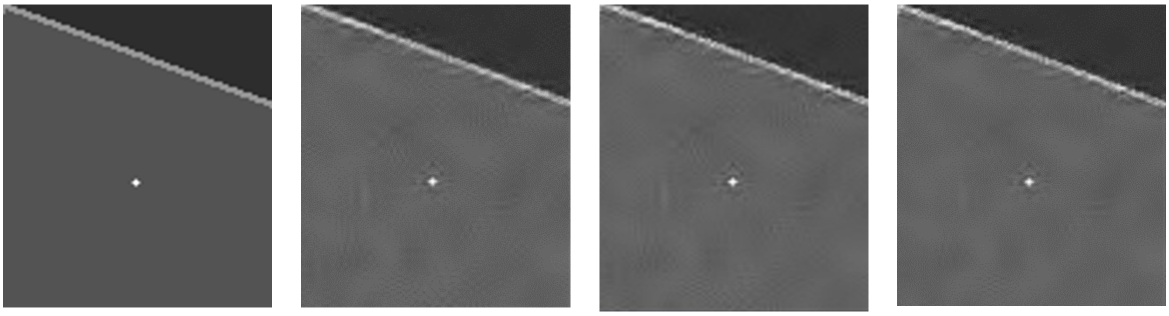

a) b) c) d)

**Fig. 5 Bright point at optimal β according to the PSNR-HVS-M metric: a) - original image; b) - original filter variant at $\beta_{optimal}^{standard}$ = 2.7; c) – modification (3) at $\beta_{optimal}^{median}$= 3; d) – modification (2) at $\beta_{optimal}^{IQR}$ = 3.2**

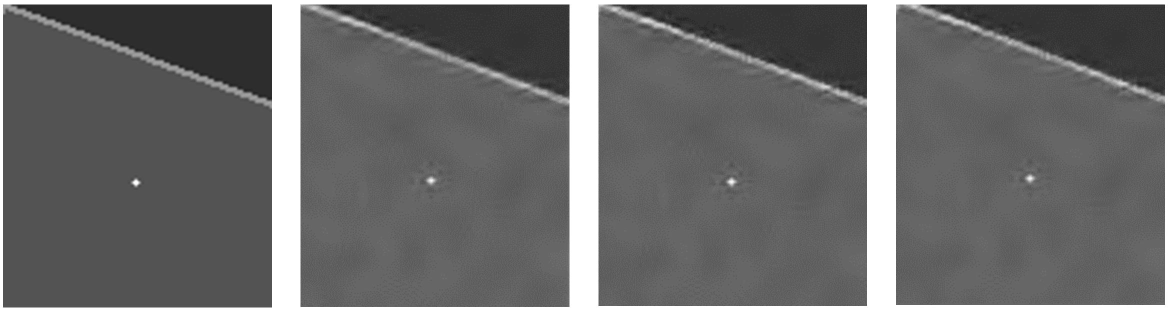

a) b) c) d)

**Fig. 6 Bright point at optimal β according to the HaarPSI metric: a) - original image; b) - original filter variant at $\beta_{optimal}^{standard}$ = 3.4; c) – modification (3) at $\beta_{optimal}^{median}$ = 3.8; d) – modification (2) at $\beta_{optimal}^{IQR}$ = 4.2**

As can be seen from Fig. 5 and Fig. 6, as β increases, the neighborhood of the bright point becomes blurred, which leads to the deterioration of the quality and coincides with the results in Fig. 2. Also in Fig. 5,c and Fig. 6,c it is noticeable that modification (3) preserves the bright point better than the original filter variant or modification (2). Now let us consider real images obtained with the Sentinel-1 system (Fig. 7).

a) b)

**Fig.7 Noise-free test images**

To these images, speckle noise with statistical ($\sigma_{\mu}^{2} = 0{,}05$) and spectral characteristics, which coincide with the noise characteristics of the Sentinel-1 system (Fig. 1,b) was added.

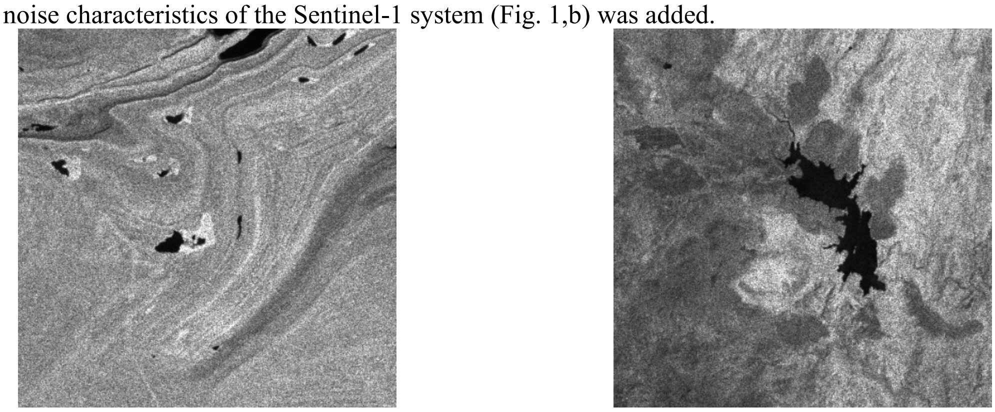

a) b)

**Fig.8 Noisy variants of images in Figures 7 a) and 7 b)**

Having filtered the image in Fig. 8,a with the original version of the filter, modification (2) and modification (3), we obtained the following graphs of dependence of the metrics on the parameter β.

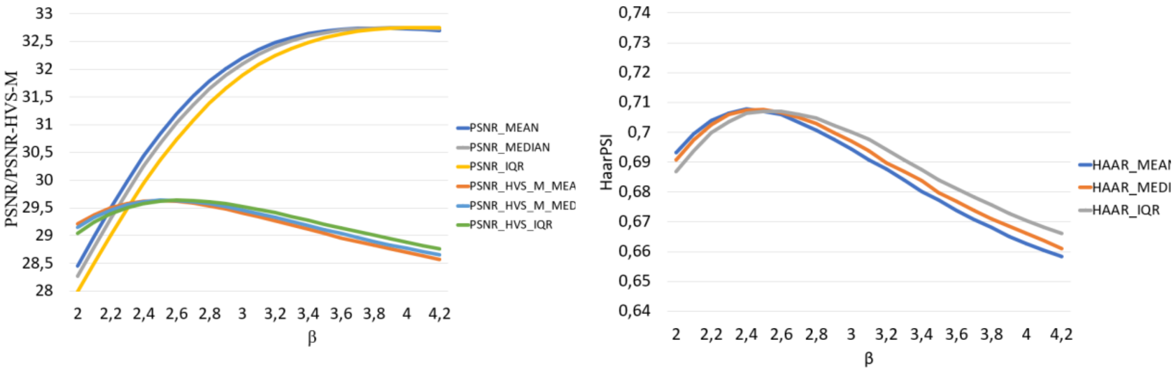


**a) b)**

**Fig. 9 - Plots of dependences of metrics values on β for the image in Fig. 8,a**

As can be seen, for each of the variants, in contrast to the synthetic image (Fig. 3, a), the optimal values of β practically coincide. Thus, according to the PSNR-HVS-M metric, the optimal β for the original filter variant and its modifications coincide and are equal to $\beta_{opt} = 2.4$. Analysis of the HaarPSI metric shows that $\beta_{opt} = 2.4$ for the original version of the filter and its modification using the median (3) for calculation, and for modification (2) $\beta_{\text{optimal}}^{\text{IQR}}$ =2.6. Based on the results, it can be seen that modification (2) allows preserving object boundaries and fine details with greater suppression of spatially correlated noise due to the largest value of the $\beta_{opt}$. Let us consider the images at the output of the filter and its modifications at optimal values of β according to the PSNR-HVS-M and HaarPSI (Fig. 10 and 11).

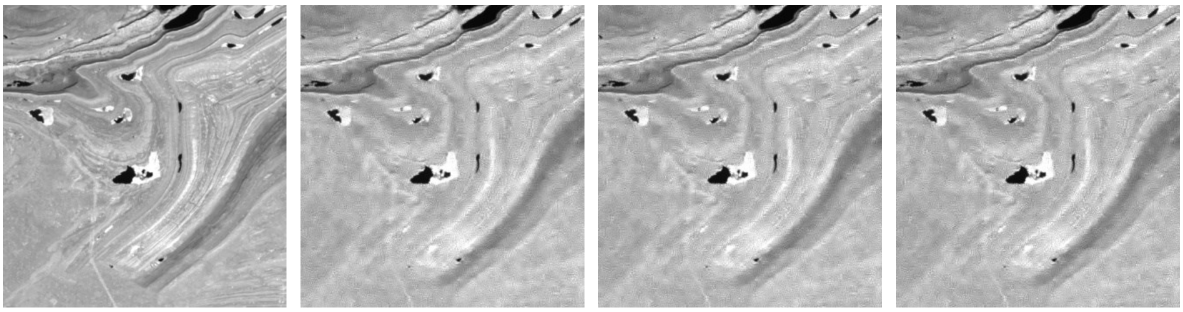

**a) b) c) d)**

**Fig. 10 Optimal output images according to the PSNR-HVS-M metric for $\beta_{opt} = 2.4$: a) - original image; b) - filter without modification; c) - filter with modification (3); d) - filter with modification (2)**

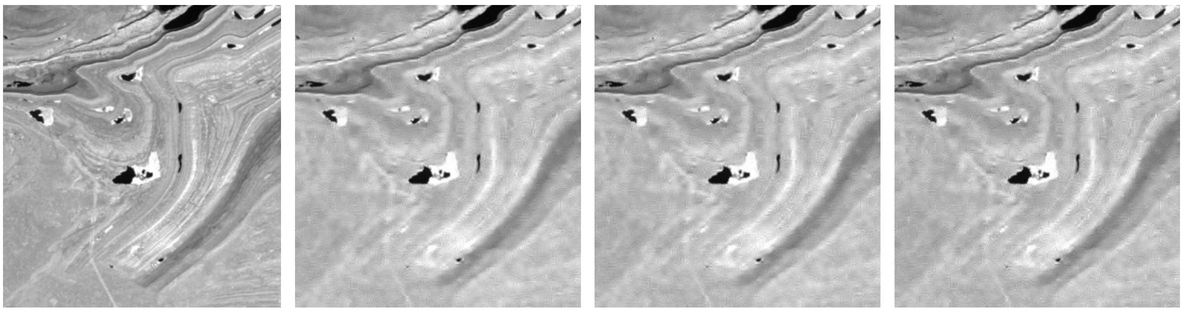

**a) b) c) d)**

**Fig. 11 Optimal output images according to the HaarPSI metric: a) - original image; b) - filter without modification, $\beta_{\text{optimal}}^{\text{standard}}$ = 2.4; c) - filter with modification (3), $\beta_{\text{optimal}}^{\text{median}}$ – 2.4; d) - filter with modification (2), $\beta_{\text{optimal}}^{IQR}$ = 2.6**

When comparing the images at the filter output at different values of β (Fig. 11), we can see that at higher values of β the noise in homogeneous areas becomes less noticeable, while small objects and edges are not blurred. Let us perform speckle suppression for the second test image (Fig. 8,b).

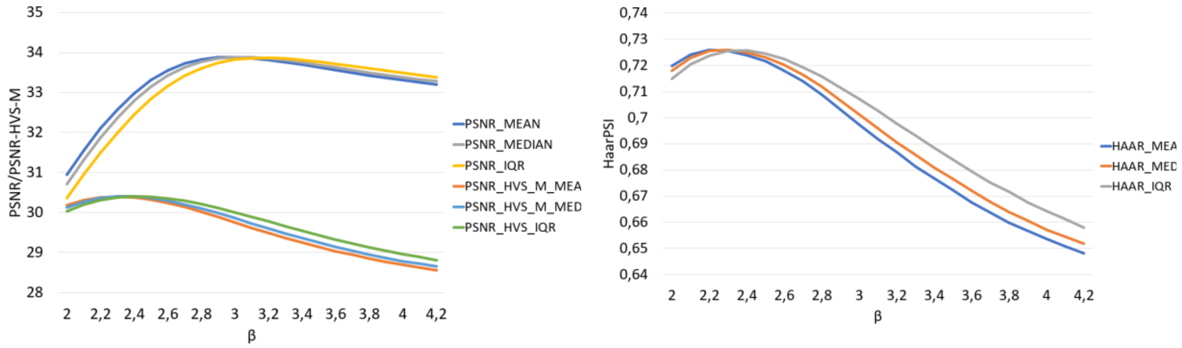


a) b)

**Fig.12 - Plots of metrics values on β for the image in Fig. 8,b**

Similar to the results obtained for speckle noise suppression in Fig. 9.a, the maximum quality for the PSNR-HVS-M is observed with the same value of β equal to $\beta_{opt}$ = 2.4 for all considered filter variants. The result of the HaarPSI metric (Fig. 8, b) is also similar to the result obtained for the previous image, $\beta_{opt}$ = 2.3 is the same for the original filter and modification (3), while for modification (2) the optimal value of the beta parameter is slightly larger and is $\beta^{IQR}_{optimal}$ = 2.4. The median filter in both cases gives a result close to the unmodified image quality at the output at the corresponding values of β. The results of image processing with the corresponding $\beta_{opt}$ are shown in Fig. 13.

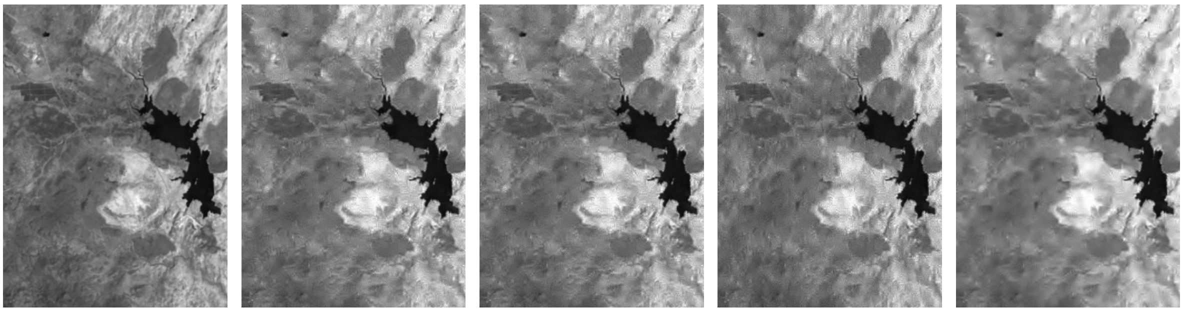

a) b) c) d) e)

**Fig. 13 Optimal output images according to the PSNR-HVS-M metric for $\beta_{opt}$ = 2.3: a) - original image; b) - filter without modification; c) - filter with modification (3); d) - filter with modification (2); e) filter with modification (2) for $\beta^{IQR}_{optimal}$ = 2.4**

## Conclusions

The influence of the choice of statistical parameter for calculating the threshold value for the DCT-SSA filter has been investigated experimentally. It is demonstrated that increasing of β causes blurring of the object edges and bright points. For the synthetic image, the modification of the filter using the median to calculate the thresholds has shown the best result, while the modification using the minimum interquantile distance shown the worst result. However, when analyzing the results for the HaarPSI metric obtained when processing real images, we found that the modification using the minimum interquantile distance allows obtaining a quality similar to the original filter and the filter using the median at large values of β. Based on the results obtained, we can conclude that replacing the statistical parameter for calculating the threshold value of the DCT-SSA filter resulted in a slight improvement in the image quality of the filter output. This proves the expediency of further search for the optimal parameter for calculating the threshold value of the DCT-SSA filter.

## References


1. Wei, S., Zeng, X., Qu, Q., Wang, M., Su, H., & Shi, J. (2020). HRSID: A high-resolution SAR images dataset for ship detection and instance segmentation. *IEEE Access, 8*, 120234–120254. https://doi.org/10.1109/ACCESS.2020.3005175
2. Singh, P., Diwakar, M., Shankar, A., Shree, R., & Kumar, M. (2021). A review on SAR image and its despeckling. *Archives of Computational Methods in Engineering, 28*, 4633–4653. https://doi.org/10.1007/s11831-021-09564-9
3. Makinen, Y., Azzari, L., & Foi, A. (2019, September 22–25). Exact transform-domain noise variance for collaborative filtering of stationary correlated noise. *Proceedings of IEEE International Conference on Image Processing (ICIP)* (pp. 185–189). https://doi.org/10.1109/ICIP.2019.8802964
4. Mullissa, A. G., Persello, C., & Tolpekin, V. (2018, July). Fully convolutional networks for multi-temporal SAR image classification. *Proceedings of the IEEE International Geoscience and Remote Sensing Symposium (IGARSS)* (pp. 6635–6638). https://doi.org/10.1109/IGARSS.2018.8518780

5. Deledalle, C. A., Denis, L., Tabti, S., & Tupin, F. (2017). MuLoG, or how to apply Gaussian denoisers to multi-channel SAR speckle reduction? *IEEE Transactions on Image Processing, 26*(9), 4389–4403. https://doi.org/10.1109/TIP.2017.2713946

6. Kupidura, P. (2016, July 12–19). Comparison of filters dedicated to speckle suppression in SAR images. *ISPRS-International Archives of the Photogrammetry, Remote Sensing and Spatial Information Sciences* (pp. 269–276). https://doi.org/10.5194/isprsarchives-XLI-B7-269-2016

7. Lee, J.-S., Wen, J.-H., Ainsworth, T. L., Chen, K.-S., & Chen, A. J. (2009). Improved sigma filter for speckle filtering of SAR imagery. *IEEE Transactions on Geoscience and Remote Sensing, 47*(1), 202–213. https://doi.org/10.1109/TGRS.2008.2002881

8. Abramov, S., Rubel, O., Lukin, V., Shelestov, A., & Lavreniuk, M. (2017, December 4). Speckle reducing for Sentinel-1 SAR data. *Proceedings of the IEEE International Geoscience and Remote Sensing Symposium (IGARSS)* (pp. 2353–2356). https://doi.org/10.1109/IGARSS.2017.8127463

9. Parrilli, S., Poderico, M., Angelino, C. V., & Verdoliva, L. (2012). A nonlocal SAR image denoising algorithm based on LLMMSE wavelet shrinkage. *IEEE Transactions on Geoscience and Remote Sensing, 50*(2), 606–616. https://doi.org/10.1109/TGRS.2011.2161586

10. Cozzolino, D., Verdoliva, L., Scarpa, G., & Poggi, G. (2020). Nonlocal CNN SAR image despeckling. *Remote Sensing, 12*(6), 1006. https://doi.org/10.3390/rs12061006

11. Kadah, Y. M., & Elnokrashy, A. F. (2024). Edge detail preservation technique for enhancing speckle reduction filtering performance in medical ultrasound imaging. *International Journal of Advanced Computer Science and Applications, 15*(2), 11.

12. Zhang, L., Mou, X., & Zhang, D. (2011). FSIM: A feature similarity index for image quality assessment. *IEEE Transactions on Image Processing, 20*, 2378–2386. https://doi.org/10.1109/TIP.2011.2109730

13. Larson, E., & Chandler, D. (2010). Most apparent distortion: Full-reference image quality assessment and the role of strategy. *Journal of Electronic Imaging, 19*(1), 011006. https://doi.org/10.1117/1.3267105

14. Xue, W., Zhang, L., Mou, X., & Bovik, A. (2014). Gradient magnitude similarity deviation: A highly efficient perceptual image quality index. *IEEE Transactions on Image Processing, 23*, 684–695. https://doi.org/10.1109/TIP.2013.2293423

15. Wang, Z., Simoncelli, E., & Bovik, A. (2003, November 9–12). Multiscale structural similarity for image quality assessment. *Proceedings of the 37th Asilomar Conference on Signals, Systems & Computers* (pp. 1398–1402).

16. Rubel, O., Lukin, V., & Egiazarian, K. (2018, October). Additive spatially correlated noise suppression by robust block matching and adaptive 3D filtering. *Journal of Imaging Science and Technology*, 12.

17. Rubel, O., Lukin, V., Krivenko, S., Pavlikov, V., Zhyla, S., & Tserne, E. (2021, September 30). Reduction of spatially correlated speckle in textured SAR images. *International Journal of Computing*, 9.

18. Rubel, O., Lukin, A., & Egiazarian, K. (2021). Selection of Lee filter window size based on despeckling efficiency prediction for Sentinel SAR images. *Remote Sensing, 13*(10), 1887.

19. Abramov S., Rubel O., Lukin V., Shelestov A., Lavreniuk M. (2017). Speckle reducing for Sentinel-1 SAR data. *Proceedings of the International Geoscience and Remote Sensing Symposium (IGARSS), Fort Worth, TX, USA, pp.* 2353-2356. https://doi.org/10.1109/IGARSS.2017.8127463

20. Kuan, D., Sawchuk, A., Strand, T., & Chavel, P. (1987). Adaptive restoration of images with speckle. *IEEE Transactions on Acoustics, Speech, and Signal Processing, 35*, 373–383.

21. Foucher, S., & López-Martínez, C. (2014). Analysis, evaluation, and comparison of polarimetric SAR speckle filtering techniques. *IEEE Transactions on Image Processing, 23*(4), 1751–1764.

22. Choi, H., & Jeong, J. (2019). Speckle noise reduction for ultrasound images by using speckle reducing anisotropic diffusion and Bayes threshold. *Journal of X-ray Science and Technology, 27*(5), 885–898.

23. Lu, B., & Ku, Y. (2010). Speckle reduction with multiresolution bilateral filtering for SAR image. *2010 International Conference on Machine Vision and Human-Machine Interface* (pp. 700–703). https://doi.org/10.1109/MVHI.2010.108

24. Oktem, R., & Ponomarenko, N. N. (2007). Image filtering based on discrete cosine transform. *Telecommunications and Radio Engineering, 66*(18), 1685–1701. https://doi.org/10.1615/TelecomRadEng.v66.i18.70

25. Huang, S., Tang, C., Xu, M., Qiu, Y., & Lei, Z. (2019). BM3D-based total variation algorithm for speckle removal with structure-preserving in OCT images. *Applied Optics, 58*, 6233–6243.

26. Chauhan, K., Chauhan, R. K., & Saini, A. (2018). Enhancement and despeckling of echocardiographic images. In *Soft Computing-Based Medical Image Analysis* (pp. 61–79). Academic Press.

27. Ponomarenko, N., et al. (2007). On between-coefficient contrast masking of DCT basis functions. *Proceedings of the Third International Workshop on Video Processing and Quality Metrics*, 4.

28. Reisenhofer, R., Bosse, S., Kutyniok, G., & Wiegand, T. (2018). A Haar wavelet-based perceptual similarity index for image quality assessment. *Signal Processing: Image Communication, 61*, 33–43. https://doi.org/10.1016/j.image.2017.11.001